Electronic Supplementary Material (ESI) for RSC Advances.
This journal is © The Royal Society of Chemistry 2015

# Supporting Information

## Graphene nanosheets decorated with ZnO nanoparticles: Facile synthesis and promising application for enhancing mechanical and gas barrier properties of rubber nanocomposites

Yong Lin, Zhikai Zeng, Jiarong Zhu, Song Chen, Xue Yuan, Lan Liu*

*College of Materials Science and Engineering, Key Lab of Guangdong Province for High Property and Functional Macromolecular Materials, South China University of Technology, Guangzhou 510640, P. R. China.*

* *Corresponding author. Tel.: +86 20 87114857; E-mail addresses: psliulan@scut.edu.cn (L. Liu).*

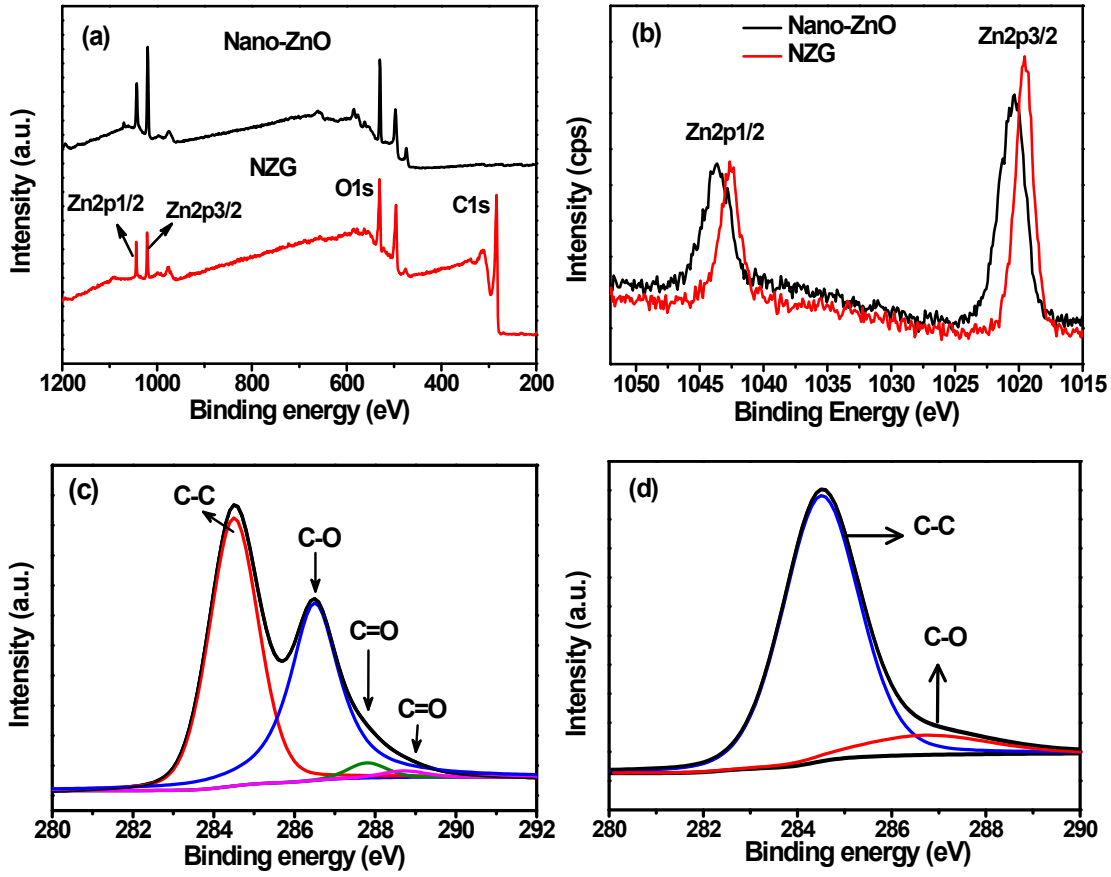


**Fig. S1**. (a) XPS survey spectra of Nano-ZnO and NZG, (b) High resolution Zn2p spectra (b) of nano-ZnO and NZG, (c) High resolution C1s spectra of GO, (d) High resolution C1s spectra of NZG.

XPS was used to investigate the chemical bonding between nano-ZnO and GE. As shown in Fig. S1(a), the XPS survey spectra show the full range of binding energy scanned from 200 to 1200 eV, which presents information on the main chemical components in the samples from the detected peaks: C1s, O1s, Zn2p. Fig. S1(b) shows the Zn2p spectrum of nano-ZnO and NZG. As for Nano-ZnO, the peaks attributed to Zn2p3/2, Zn2p1/2 appear at 1020.4, 1043.7 eV, respectively. In comparison, the peaks corresponding to Zn2p3/2 and Zn2p1/2 shifts to 1019.4 eV and 1042.6 eV, respectively. This shifts in the binding energies for Zn2p3/2 and Zn2p1/2 demonstrates that GE could be effectively functionalized by coupling with ZnO[a,b].

As shown in Fig. S1(c), the high resolution C1s spectra of GO presents four types of carbon atoms, namely the non-oxygenated ring C (284.5 eV), the C atom in the C-O bond (286.7 eV), the carbonyl C (287.8 eV) and the carboxylate C in O-C=O (288.7 eV).[c,d] As for NZG (Fig. S1(d)), the peak intensity of C-O bond are much weaker than those in GO, and other peaks of carbon atoms binding to oxygen also disappear, suggesting most of oxygen-containing functional groups have been removed after reduction.

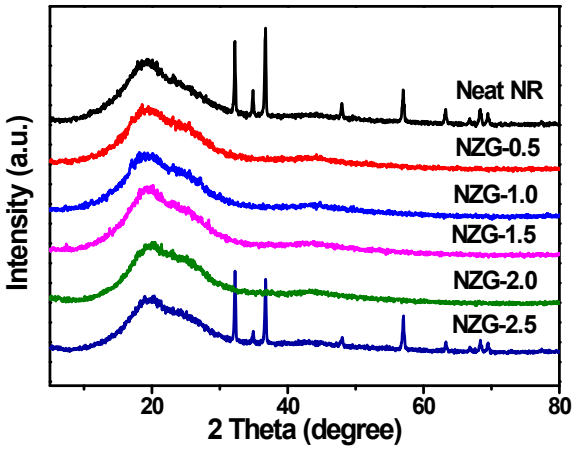


**Fig. S2.** XRD patterns of NR/NZG nanocomposites with different of NZG contents.

As shown in Fig. S2, a broad diffraction peak is observed for neat NR, an indication of a noncrystalline structure. Noticeably, the characteristic peaks of ZnO are also detected in the composites, strongly suggesting that excessive use of conventional ZnO as an activator is provided for the vulcanization process in term of the traditional basic recipe. It can also be found that only the diffraction peak indexed to noncrystalline structure of NR composites appears for NR/NZG nanocomposites with low NZG content (□2.5 phr), all without the characteristic peaks corresponding to graphite and ZnO, revealing that nano-ZnO decorated on the GE sheets not only efficiently participates in the vulcanization, but also facilitates the GE sheets well-dispersed in the matrix. Nevertheless, with the inclusion of 2.5 phr NZG into the matrix, the diffraction peaks ascribed to ZnO

are observed for NR/NZG-2.5 nanocomposite, which is indicative of that the excessive NZG were used for the vulcanization. Therefore, it is believed that NZG with a low content has a higher vulcanization efficiency compared with 5 phr conventional ZnO.

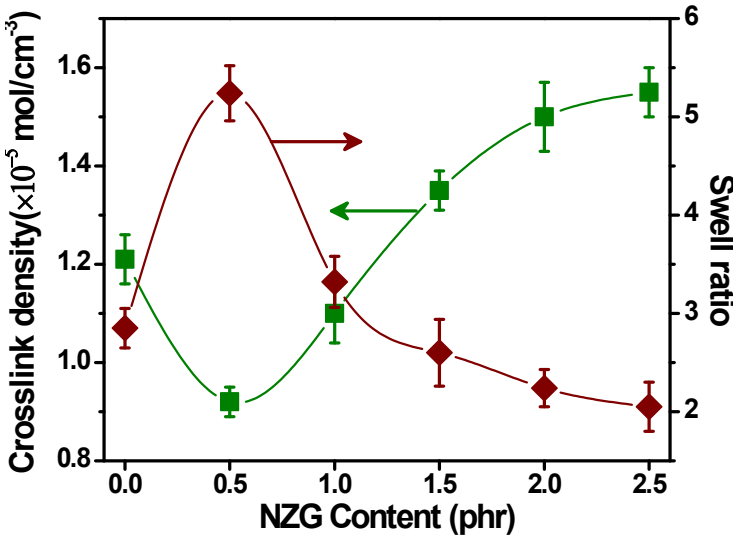


**Fig. S3.** Crosslink density analysis of neat NR and NR/NZG nanocomposites.

The crosslink density and swelling ratio of NR/NZG nanocomposites were recorded and the results are present in Fig. S3. With increasing NZG content, the crosslink density increases significantly whereas the swelling ratio decreases continuously. For instance, the crosslink density of NR/NZG-2.5 nanocomposite increases by 28.1% over that of neat NR, and the swelling ratio of the nanocomposite decreases by 27.7% below that of neat NR. To explain this phenomenon, one should have an insight into the vulcanization efficiency of nano-ZnO. It can be deduced that the excellent surface area of nano-ZnO would provide the maximum potential of the contacts between nano-ZnO particles and the rubber additives in the vulcanization, efficiently promoting the vulcanization and dramatically enhancing the constitution of crosslink network. Meanwhile, the improvement in the crosslink density is generally observed by incorporating GE into the matrix owing to the introduced physical and chemical crosslink points[c-e].

As observed, with the low NZG content (□1.5 phr), NR/NZG nanocomposites have a lower

crosslink density compared with neat NR activated by 5 phr conventional ZnO. This is attributed to that low nano-ZnO content at a low NZG content significantly limits the formation of the intermediates, hindering the vulcanization. As the concentration of the curing package relative to the NR is identical for all the nanocomposites, and therefore the activated efficiency of nano-ZnO and the incorporation of GE are responsible for the enhancement of the crosslink density of NR/NZG nanocomposites.

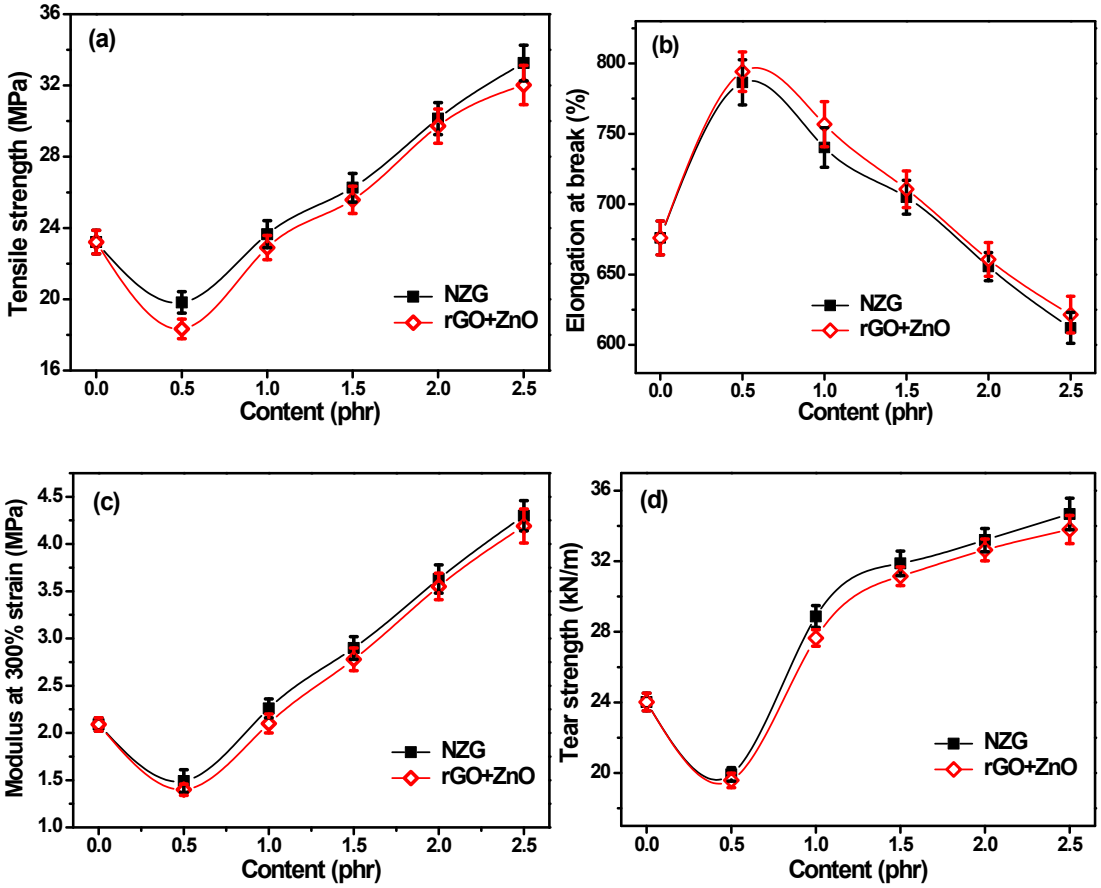


**Fig. S4.** Comparison of mechanical properties of NR/NZG and NR/rGO/ZnO nanocomposites.

For the further comparison, the mechanical properties of NR composites prepared by physically adding rGO and ZnO (NR/rGO/ZnO composites) were provided in Fig. S4 of supporting information. It is clearly seen that NR/NZG nanocomposites show the improved mechanical properties to those of NR/rGO/ZnO composites at the same filler content. This phenomenon is attributed to that a simple physical mixing for adding rGO and nano-ZnO into the NR matrix may lead to the tendency of the monolayeric graphene sheet to agglomerate into multilayeric graphite. And the agglomeration of nano-

ZnO particles may be more serious, greatly affecting the vulcanization.

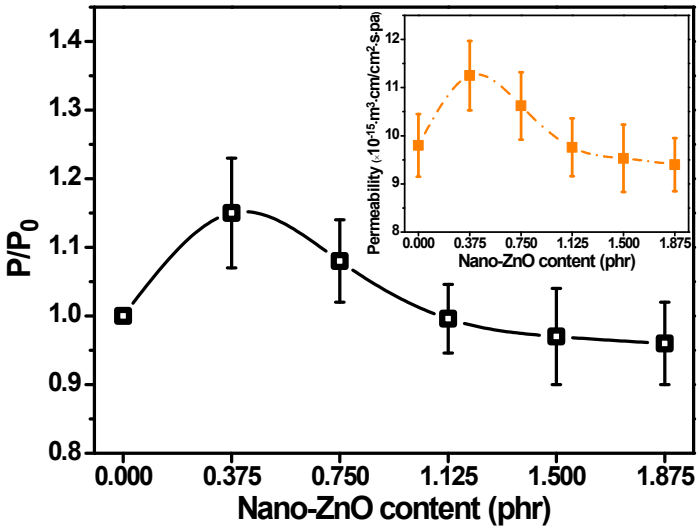


**Fig. S5** Nitrogen permeability of NR/Nano-ZnO nanocomposites normalized by that of neat NR. The upper inset shows the absolute values of nitrogen permeability.

In order to further verify the effect of NZG on the permeability of NR nanocomposites, the permeabilities of NR/Nano-ZnO nanocomposites were recorded for the comparison. As shown in Fig. S5, with the inclusion of nano-ZnO with low content (< 1.125 phr) into the matrix, a significant increase in the permeability for NR/Nano-ZnO nanocomposites was observed as compared with that of neat NR. For further adding higher content of nano-ZnO, it exhibits a weak reduction in the gas permeability of NR nanocomposites. These results may be due to that the moderate content of nano-ZnO can efficiently perfect the crosslinked network, further improving the permeability of NR nanocomposites.

**Table S1.** Specific surface areas of the conventional ZnO, Nano-ZnO and NZG.

| Sample | Specific surface areas ($m^2/g$) |
|---|---|
| Conventional ZnO | 6.046 |
| Nano-ZnO | 31.253 |

| | | |
|---|---|---|
| NZG | - | 35.566 |

As shown in Table S1, the specific surface areas of conventional ZnO is only 6.046 $m^2/g$, while the specific surface areas of NZG is up to 35.566 $m^2/g$. The large surface area is more conducive to promote the formation of the zinc salts of stearic acids, and solubilize those insoluble accelerators to form the actual catalyst for vulcanization process. Noteworthily, the specific surface areas of NZG (35.566 $m^2/g$) is larger than that of Nano-ZnO (31.253 $m^2/g$), directly indicating a significantly higher aggregation tendency for nano-ZnO. That is to say, ZnO nanoparticles decorated onto the GE sheets can reduce the aggregation tendency to a certain extent. Therefore, NR/NZG nanocomposites filled with lower NZG content can exhibit superior mechanical properties to those of neat NR and NR/Nano-ZnO nanocomposites.

**References**


a J. L. Wu, X. P. Shen, L. Jiang, K. Wang and K. M. Chen, *Appl. Surf. Sci.,* 2010, **256**, 2826-2830.

b R. C. Wang, Y. C. Chen, S. J. Chen and Y. M. Chang, *Carbon*, 2014, **70**, 215-223.

c H. F. Yang, C. S. Shan, F. H. Li, D. X. Han, Q. X. Zhang and L. Niu, *Chem. Commun.*, 2009, **26**, 3880-3882.

d Y. Wang, Z. Shi and J. Yin, *ACS Appl. Mater. Interfaces* 2011, **3**, 1127-1133.

e Z. Wang, J. Liu, S. Wu, W. Wang and L. Zhang, *Phys. Chem. Chem. Phys.*, 2010, **12**, 3014-3030.

f Y. Zhan, J. Wu, H. Xia, N. Yan, G. Fei and G. Yuan, *Macromol. Mater. Eng.*, 2011, **296**, 590-602.

g J. R. Wu, W. Xing, G. S. Huang, H. Li, M. Z. Tang, S. D. Wu and Y. F. Liu, *Polymer*, 2013, **54**, 3314-3323.